

Surface morphology and characterization of thin graphene films on SiC vicinal substrate

J. Penuelas,¹ A. Ouerghi,^{2,*} D. Lucot,² C. David,² J. Gierak,² H. Estrade-Szwarczopf,¹ and C. Andreazza-Vignolle¹

¹Centre de Recherche sur la Matière Divisée, UMR 6619, Université d'Orléans–CNRS, 1 bis, rue de la Férollerie, 45071 Orléans Cedex, France

²Laboratoire de Photonique et Nanostructure–CNRS, Route de Nozay, 91460 Marcoussis, France

(Received 28 July 2008; revised manuscript received 4 November 2008; published 21 January 2009)

In this Brief Report we present a study of a 6H-SiC(0001) vicinal substrate annealed at various temperatures under ultrahigh vacuum. By combining x-ray photoelectron spectroscopy and atomic force microscopy, we investigated the morphology and the chemical surface changes accompanying the formation of graphene sheets. After annealing at 1100 °C step/terrace structures of the SiC substrate are clearly identified and a terrace widening is observed due to step bunching up. At 1300 °C approximately two graphene layers are formed and the surface steps completely disappear.

DOI: 10.1103/PhysRevB.79.033408

PACS number(s): 68.55.A–, 68.37.Ps, 79.60.–i

The recent discovery of novel electronic properties such as ambipolar field effect¹ or room-temperature (RT) quantum Hall effect² in mechanically exfoliated graphene sheets has initiated intense exploration into this new two-dimensional (2D) material.³ This led to a resurgence of interest in graphite epitaxially grown by heating hexagonal silicon carbide crystals,^{4,5} which may provide opportunities for large-scale integration of graphene in future nanoelectronics. One advantage of graphene/SiC is that the thickness of graphene grown on SiC can be precisely controlled to be either single or multilayered [called few layers graphene (FLG)] depending on growth parameters.^{6,7} Future applications involving patterning of graphene/SiC require understanding the structure and the growth mechanisms of graphene layers on SiC substrate. These layers are grown on a complex SiC precursor layer whose geometric structure is not yet fully clear,⁸ but recent studies seem to show that graphitization on Si-terminated face occurs on a $(6\sqrt{3} \times 6\sqrt{3})$ reconstruction strongly bound to the underlying Si atoms.⁹ Chemically and structurally abrupt and defect-free interfaces are required in such devices, which makes the surface preparation of the SiC substrate important. The growth of graphene on SiC can be achieved either on the (0001) (silicon-terminated) or on the (000 $\bar{1}$) (carbon-terminated) faces of 4H- and 6H-SiC crystals by annealing at temperature above 1300 °C in ultrahigh vacuum (UHV). The aim of this experiment was to find out whether it is possible to prepare a stepped graphene surface and create electron gases, with a significant one-dimensional (1D) or 2D lateral potential modulation by using a stepped SiC substrate.¹⁰ An essential advantage of using organized growth on vicinal substrates off (0001) is that the low-dimensional structures are obtained in a single technological step (epitaxial graphene). The effects of substrate temperature together with the structural and chemical evolutions of this nanostructured graphene/SiC(0001) were characterized by means of atomic force microscopy (AFM) and x-ray photoelectron spectroscopy (XPS). Particular attention is paid to the evolution of the surface morphology (terrace; step) during annealing at various temperatures.

FLG growth was carried out *in situ* in ultrahigh vacuum on *n*-type Si-terminated 6H-SiC(0001) (on 3; 5° off) surface is toward $[11\bar{2}0]$ by thermal desorption of silicon at high

temperatures.^{4,5} Samples were first *ex situ* chemically cleaned including trichloroethylene, acetone, and methanol; ultrasonic bath was followed by 50% high-frequency (HF) etching. The sample then was immediately introduced into UHV and treated *in situ* by resistive heating. After degassing for 8 h at 600 °C, the sample was annealed for 5 min at different temperature between 800 °C and 1300 °C by steps of 50 °C under a base pressure lower than 10^{-9} mbar. The graphene thickness can be tailored by controlling the temperature and, the annealing time. In what follows we describe detailed structural studies conducted using *ex-situ* atomic force microscopy (AFM nanoscope III digital instrument) working in tapping mode (amplitude=4 nm, resonance frequency=1 Hz, and rows and columns=512). After annealing, the samples were cooled down to room temperature and transferred under UHV from the growth chamber to the XPS analysis chamber. XPS experiments were carried out on a VG ESCALAB 250 system using Mg K α monochromatized radiation of 1253.6 eV and a hemispherical energy analyzer. Spectra were collected either in a normal-emission mode or under grazing conditions; in the latter case, the angle between the normal to the sample surface and the lens axis is set to be 70° in order to collect information from the thinner surface layer. With Mg K α source, the total instrumental energy resolution was about 0.4 eV. XPS analysis was performed at room temperature and data fitting done with VG software described in Ref. 11. The software employs classical parameters such as intensity, binding-energy, linewidth, and Gaussian or Lorentzian mixing ratio for symmetrical lines, full width at half maximum (FWHM) values, and the exponential tail parameters for asymmetrical lines.

Before going into details of sublimation phenomenology, let us first have a look at the organization of pristine SiC surface. Figure 1 shows the structure evolution of the SiC during UHV annealing for three temperatures. To allow AFM investigation of SiC sublimation, SiC surface was stabilized at 900 °C in UHV and further slowly annealed with different temperature steps. Figure 1(a) shows an AFM image of SiC surfaces after annealing at 1100 °C. It was clearly observed that terraces on the SiC surface were atomically flat and also these terraces were separated by fairly straight step edges. The average terrace width was 24 nm. It was found that the smooth microsteps were formed at the step edges with an

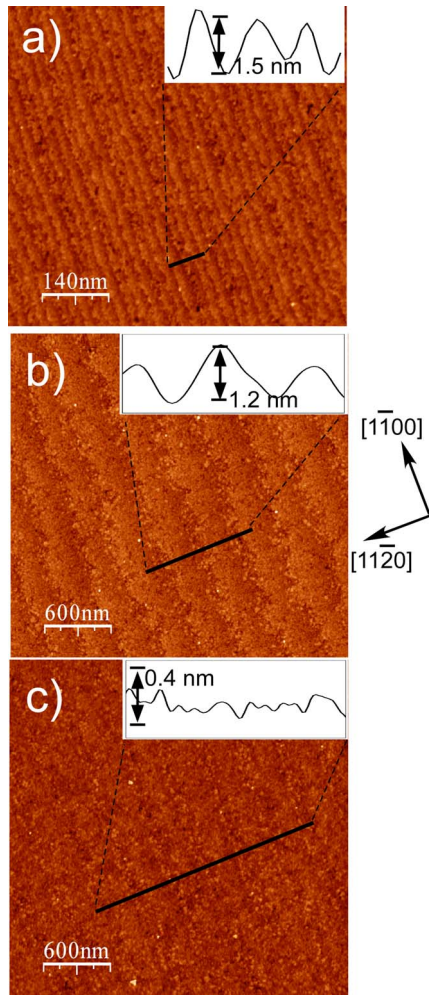


FIG. 1. (Color online) A series of the AFM images and line sections (insert) displaying the surface evolution of the SiC during UHV annealing: (a) AFM images of the SiC at 1100 °C, (b) 1200 °C, and (c) 1300 °C.

average height of 1.5 nm, corresponding to six SiC bilayers. Terrace widening probably resulted from the microstep formation induced by the step bunching.¹² Step bunching was also observed and partly explained in terms of etching kinetics and surface energies by Nakamura *et al.*¹³ Ohtani *et al.*¹⁴ suggested that regular step ordering on on-axis SiC surfaces is related to short-range order step-step interactions. Figure 1(b) presents large-scale AFM image of the surface after annealing at 1200 °C. A characteristic feature of this sample was the appearance of terraces along the $[1\bar{1}00]$ direction. The average terrace width was drastically widened up to 370 nm if compared with the original width of SiC terrace (about 24 nm). Terrace widening resulted from the multistep formation induced by step bunching up (0.9–1.2 nm). The steps are no longer atomically smooth as they were probably perturbed by the nucleation of the first carbon layer. When this sample is further heated to 1300 °C, the SiC steps completely disappear. The flat surface may then correspond to a completely graphenic surface [Fig. 1(c)]. This claim for getting a flat graphene surface is in agreement with (i) previous observation of thermal Si desorption⁵ and with (ii) the ab-

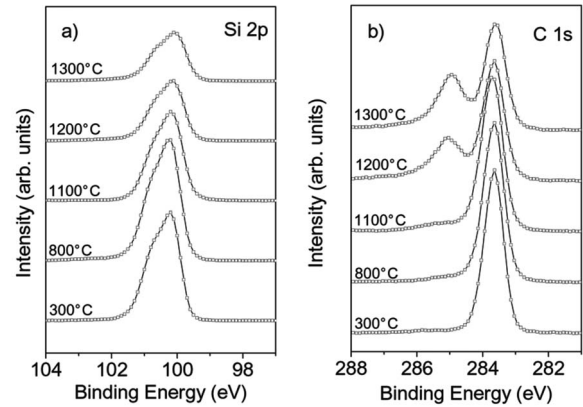


FIG. 2. (a) Si 2p XPS spectra of 6H-SiC(0001) surfaces; (b) C 1s XPS spectra of 6H-SiC(0001) surfaces annealed at different substrate temperatures at normal incidence.

sence of residual step afterward. A possible reason for the surface flatness is that the new layer covers previous steps. Probably, graphene sheets, which are only few nanometers thick, are now located on the top of step SiC substrate. Similar surface was also observed for graphene epilayers on Si-terminated SiC(0001)¹⁵ by low energy electron diffraction.

In order to check the formation of graphene epilayers, XPS measurements were carried out as a function of the substrate annealing temperature. Figures 2(a) and 2(b) present the respective XPS spectra of the Si 2p (the Si 2p^{3/2} and Si 2p^{1/2} are not completely resolved) and C 1s core levels obtained for samples annealed at different substrate temperatures. Obviously, those treatments induce significant changes in the XPS spectra. First of all, a decrease in the Si 2p intensity is observed compared to the C 1s intensity, showing clearly a decrease in the relative concentration silicon/carbon with the annealing temperature. This decrease is probably due to the fast thermal desorption of Si. At 300 °C, the position of the Si 2p peak is centered at 100.2 eV, which is relevant to the value for elemental SiC. The absence of any additional peak indicates that no Si oxidized species are present in the sample. These oxidized species, if present, would appear at higher binding energies between 105 and 106 eV.¹⁶ The evolution of the C 1s line shape with temperature [see Fig. 2(b)] reveals significant changes. At 300 °C the C 1s line shape is characteristic of carbon in SiC structure located around 283.65 eV, in agreement with other experiments.⁹ Annealing at 800 °C was performed without any visible change in the C 1s line shape; at 1100 °C a small contribution at around 285.2 eV becomes visible, which may be attributed to the beginning of surface reconstruction.^{9,15} After annealing at 1200 °C (1300 °C), a new peak is observed which relates to a new chemical organization of the surface. This peak increases with the temperature. Two measurements were performed at $\varphi=0^\circ$ and $\varphi=70^\circ$ extraction angle in order to identify surface or bulk-related components of the sample after annealing at 1300 °C [see Fig. 3(a)]. At grazing detection ($\varphi=70^\circ$), the intensity of the 285.2 eV component is stronger than that of 283.6 eV one, whereas at $\varphi=0^\circ$, its intensity is weaker than that of the 283.6 eV. Evidently, the 283.6 eV component can be classically attributed

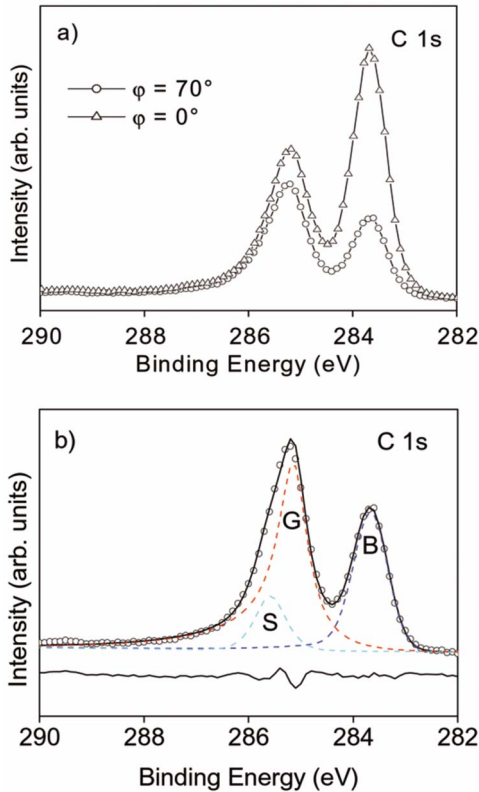


FIG. 3. (Color online) (a) C 1s XPS spectra of 6H-SiC(0001) surfaces annealed at 1300 °C at normal incidence and grazing incidence; (b) XPS spectra of the C 1s core level from the SiC surfaces annealed at 1300 °C at grazing incidence ($\varphi=70^\circ$); for each spectrum we give the experimental data after background subtraction and the decomposition with bulk and two surfaces components identified by *B*, *G*, and *S*, respectively.

to the bulk-related SiC located under a superficial carbon layer responsible for the 285.2 eV component of the spectrum. We ascribed this new surface component peak at 285.2 eV to FLG formation. The graphitization of the SiC surface at high temperature was necessarily accompanied by the evaporation of silicon atoms from the bulk. The experimental C 1s spectra and their fitting are reported in Fig. 3(b) for the annealing surface at 1300 °C at grazing incidence ($\varphi=70^\circ$). Raw data represented by black dots are shown together with the results of the curve fitting of the C 1s spectra in Fig. 3(b). Using asymmetrical shape for the graphene component, three contributions have to be considered to obtain consistent fits using a least-square fitting procedure:¹⁷ the small (*S*) component located at 285.9 eV (FWHM=0.78), the stronger one (*G*) at 285.1 eV (FWHM=0.65), and the bulk (*B*) component at 283.6 eV (FWHM=0.73). These doublets (*S* and *G*) can be, respectively, ascribed to surface reconstruction and to graphene. No other chemically shifted peak is needed to fit the spectrum. These results indicate that the evaporation of silicon atoms from the bulk started at 1200 °C and it is complete at 1300 °C. In order to estimate the thickness of the carbon multilayer that gives rise to *G* and *S*, we use a simple simulation of the exponential decay for the bulk (*B*) contribution as a function of the surface covering (the *G* and *S* contributions). Assuming homogeneous two-dimensional

graphene growth and equal *C* concentrations in the three phases *B*, *S*, and *G*, using a simple attenuation model with a graphene layer on top of the bulk SiC, we can estimate the thickness of the graphene using

$$\frac{I_{\text{SiC graphene}}}{I_{\text{SiC bulk}}} = \exp\left(-\frac{d}{\lambda \cos \varphi}\right),$$

where $I_{\text{SiC graphene}}$ is the normalized peak area intensity of the Si 2*p* peak for graphene sample, $I_{\text{SiC bulk}}$ is the normalized peak area intensity of the Si 2*p* peak for bulk SiC, d is the total (*S*+*G*) carbon layer thickness in nanometer, and λ is the electron escape depth estimated at 1.8 nm and assumed to be equal in both *S* and *G* phases. The ratio of the measured intensities of the peak area for the components *G*/*B* and *S*/*B* fit well with an exponential decay of roughly 2 ML of carbon covering. The other surface contribution (*S*) corresponds to less than 0.6 ML. Thus, the carbon coverage deduced by XPS corroborates the steps (0.9 nm) of the surface observed by AFM. The origin of the *S* component is attributed to *sp*²-bonded C atoms in the reconstructed layer.¹⁸ Emtsev *et al.*⁹ predicted that the concentration of atoms responsible for the *S* component also remains constant even for a film thickness greater than 3 ML.

We now discuss briefly why such graphene surface is obtained after the cycle of SiC sublimation. First of all, at 1200 °C all the Si atoms are evaporated from the surface leaving an uncovered carbon layer. Varchon *et al.*¹⁹ and Mat-tausch *et al.*⁸ recently performed density-functional theory (DFT) calculations on 4H-SiC(0001) and 6H-SiC, deducing a strong bond between the substrate and the first all-carbon layer; it is only the second carbon layer that exhibits true graphene properties. These results also suggested the presence of charge transfer that depends on the interface geometry, causing the graphene to be *n* doped. They showed that the first carbon layer is covalently bound to the substrate and it is not responsible for the graphene-type electronic spectrum. Moreover the properties of the freestanding graphene only appear with the second carbon layer, which exhibits a weak van der Waals bonding to the underlying structure. Our core-level spectra show clear evidence of surface graphitization since the *G* component is the strongest in the surface-sensitive spectrum and it appears at the same location as the graphitic C 1s peak. We obtain a thickness of 0.65 nm at $\varphi=70^\circ$, which corresponds to two graphene monolayers. The variation in relative strength of the additional *S* component compared to the *G* and *B* components indicates that there are additional carbon sites in a region underneath the graphitic surface carbon, but on top of the bulk. Quite complex structural modifications during the $6\sqrt{3} \times 6\sqrt{3}$ transformation to graphene layer were recently reported in a scanning tunneling microscopy study.²⁰⁻²² Therefore, desorption of at least three Si layers would be required to form a carbon-rich interlayer and graphene bilayer via the detachment of carbon atom, diffusion, and nucleation. In other words, even though the progressive diffusion of carbon from bulk to the surface continues consuming the SiC substrate, the structure of the interface between the SiC(0001) surface and the FLG remains identical to that of the $6\sqrt{3} \times 6\sqrt{3}$ reconstructed layer

formed during the initial stage.⁹ Physical appearance suggests that graphitization starts from the step edges and propagates gradually to the center of the terrace.²³ Indeed, C atoms at kinks and step edges have a lower coordination number and bond breaking may occur more easily there, successively inducing carbon atom detachment, diffusion, and graphitization at 1300 °C. The first carbon layer appears at the step edges at about 1200 °C, and, after annealing at higher temperature (1300 °C), the surface area covered by the first carbon layer increases. When the diffusion length of an adatom is large in comparison to the terrace width, a step flow growth mode results: the layer grows by the advance of steps not by island nucleation. Apparently, a carpetlike growth mode occurs during the growth of the graphene layer, although we cannot say explicitly which of the different preparation steps is involved.

In summary we have investigated the morphology and the

chemical structure of FLGs (two layers) grown on the 6H-SiC(0001) vicinal substrate by graphitization under UHV by AFM and XPS techniques. It was found that the desorption of at least three Si layers is needed to successively induce the detachment of a carbon atom, diffusion, and graphitization at 1300 °C. The first carbon layer appears at the step edges at about 1200 °C, and the area of the surface covered by the first carbon layer increases after annealing at higher temperature (1300 °C). Real-space observations reveal that the SiC steps completely disappear, and the surface corresponds then to a completely graphenic one, which is in agreement with previous structural studies.

The authors thank B. Etienne, P. Andreatza, R. Mysyk, and R. Benoit for fruitful and stimulating discussions.

*ouergchi@lpn.cnrs.fr

- ¹K. S. Novoselov, A. K. Geim, S. V. Morozov, D. Jiang, Y. Zhang, S. V. Dubonos, I. V. Grigorieva, and A. A. Firsov, *Science* **306**, 666 (2004).
- ²K. S. Novoselov, Z. Jiang, Y. Zhang, S. V. Morozov, H. L. Störmer, U. Zeitler, J. C. Maan, G. S. Boebinger, P. Kim, and A. K. Geim, *Science* **315**, 1379 (2007).
- ³K. S. Novoselov, D. Jiang, F. Schedin, T. J. Booth, V. V. Khotkevich, S. V. Morozov, and A. K. Geim, *Proc. Natl. Acad. Sci. U.S.A.* **102**, 10451 (2005).
- ⁴A. Charrier, A. Coati, T. Argunova, F. Thibaudau, Y. Garreau, R. Pinchaux, I. Forbeaux, J.-M. Debever, M. Sauvage-Simkin, and J.-M. Themlin, *J. Appl. Phys.* **92**, 2479 (2002).
- ⁵C. Berger, Z. Song, X. Li, X. Wu, N. Brown, C. Naud, D. Mayou, T. Li, J. Hass, A. N. Marchenkov, E. H. Conrad, P. N. First, and W. A. de Heer, *Science* **312**, 1191 (2006).
- ⁶W. A. de Heer, C. Berger, X. Wu, P. N. First, E. H. Conrad, X. Li, T. Li, M. Sprinkle, J. Hass, M. L. Sadowski, M. Potemski, and G. Martinez, *Solid State Commun.* **143**, 92 (2007).
- ⁷J. Hass, F. Varchon, J. E. Millan-Otoya, M. Sprinkle, N. Sharma, W. A. de Heer, C. Berger, P. N. First, L. Magaud, and E. H. Conrad, *Phys. Rev. Lett.* **100**, 125504 (2008).
- ⁸A. Mattausch and O. Pankratov, *Phys. Rev. Lett.* **99**, 076802 (2007).
- ⁹K. V. Emtsev, F. Speck, T. Seyller, L. Ley, and J. D. Riley, *Phys. Rev. B* **77**, 155303 (2008).
- ¹⁰T. Mélin and F. Laruelle, *Phys. Rev. Lett.* **81**, 4460 (1998).
- ¹¹P. M. A. Sherwood, in *Practical Surface Analysis*, 2nd ed., edited by D. Briggs and P. M. Seah (Wiley, New York, 1990), pp. 572–575.
- ¹²H. Nakagawa, S. Tanaka, and I. Suemune, *Phys. Rev. Lett.* **91**, 226107 (2003).
- ¹³S. Nakamura, T. Kimoto, H. Matsunami, S. Tanaka, N. Teraguchi, and A. Suzuki, *Appl. Phys. Lett.* **76**, 3412 (2000).
- ¹⁴N. Ohtani, M. Katsuno, J. Takahashi, H. Yashiro, and M. Kanaya, *Phys. Rev. B* **59**, 4592 (1999).
- ¹⁵Th. Seyller, K. V. Emtsev, K. Gao, F. Speck, L. Ley, A. Tadich, L. Broekman, J. D. Riley, R. C. G. Leckey, O. Rader, A. Varykhalov, and A. M. Shikin, *Surf. Sci.* **600**, 3906 (2006).
- ¹⁶L. Simon, L. Kubler, A. Ermolieff, and T. Billon, *Phys. Rev. B* **60**, 5673 (1999).
- ¹⁷Asymmetry parameter values of 0, 0.03, and 0.1 were found to produce best fits to the spectra recorded from, respectively, the B, G, and S peaks.
- ¹⁸L. I. Johansson, F. Owman, and P. Martensson, *Phys. Rev. B* **53**, 13793 (1996); Z. H. Ni, W. Chen, X. F. Fan, J. L. Kuo, T. Yu, A. T. S. Wee, and Z. X. Shen, *ibid.* **77**, 115416 (2008) and references therein.
- ¹⁹F. Varchon, R. Feng, J. Hass, X. Li, B. N. Nguyen, C. Naud, P. Mallet, J. Y. Veuillen, C. Berger, E. H. Conrad, and L. Magaud, *Phys. Rev. Lett.* **99**, 126805 (2007).
- ²⁰P. Lauffer, K. V. Emtsev, R. Graupner, Th. Seyller, L. Ley, S. A. Reshanov, and H. B. Weber, *Phys. Rev. B* **77**, 155426 (2008).
- ²¹P. Mallet, F. Varchon, C. Naud, L. Magaud, C. Berger, and J. Y. Veuillen, *Phys. Rev. B* **76**, 041403(R) (2007).
- ²²F. Varchon, P. Mallet, J.-Y. Veuillen, and L. Magaud, *Phys. Rev. B* **77**, 235412 (2008).
- ²³J. B. Hannon and R. M. Tromp, *Phys. Rev. B* **77**, 241404(R) (2008); Siew Wai Poon, Wei Chen, Eng Soon Tok, and Andrew T. S. Wee, *Appl. Phys. Lett.* **92**, 104102 (2008).